



**Received:** 20 February, 2021

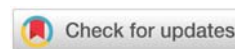
**Accepted:** 29 March, 2021

**Published:** 30 March, 2021

**\*Corresponding author:** Tugba Tugsuz, Department of Chemistry, Hacettepe University, Beytepe, Ankara 06800, Turkey, E-mail: [ttugsuz@hacettepe.edu.tr](mailto:ttugsuz@hacettepe.edu.tr); [tugba99@yahoo.com](mailto:tugba99@yahoo.com)

**Keywords:** Indigo; Indigoids; Borophene; DFT; TD-DFT

<https://www.peertechzpublications.com>



## Research Article

# A Theoretical Study on the Optical Spectroscopic Properties of Indigoids@B<sub>36</sub>

Tugba Tugsuz\*

Department of Chemistry, Hacettepe University, Beytepe, Ankara 06800, Turkey

## Abstract

Indigoids represent a family of environmentally friendly organic semiconductor materials. In this study, we aim to fine-tune the optoelectronic properties and semiconductor performance of indigoids by careful choice of the functional groups. We used Density Functional Theory (DFT) to predict the electron transport behavior of indigoids by calculating their electronic properties. The time-dependent DFT (TD-DFT) method was employed to explore the absorption spectra properties of indigo and indigoid molecules. To improve the performance of organic semiconductors, we modeled indigoids on borophene cluster. Using TD-DFT method, the absorption properties were predicted. The maximum absorption for the complex corresponding to the transition between Highest Occupied Molecular Orbital (HOMO) and Lowest Unoccupied Molecular Orbital (LUMO) showed a charge transfer transition as the electron density of the HOMO is located on the borophene and that of the LUMO on indigo and indigoids. The presence of charge transfer peaks of the absorption spectrum, the indigo and indigoids@B<sub>36</sub> complexes were found as suitable for optoelectronic devices.

## Introduction

Optoelectronics have a strong effect on the different areas of technology. The electricity is transmitted by means of optoelectronic devices that can provide wireless electricity transmission with the help of light. An optoelectronic device includes various semiconductor alloys that lay on substrates. Optoelectronics technology after studies concerning cost reduction, performance improvement and large volume manufacturing, will shape the future.

Recently, transistor properties of several halogen-substituted indigoids have been reported [1-4]. These molecules are of interest because of the minimal molecular structure consisting of electron-donating nitrogen atoms, working as a donor and electron withdrawing carbonyl groups, as an acceptor. Due to their small energy gap, long wavelength absorption is related to the ambipolar transport. Glowacki and co-workers reviewed the history of indigo and its derivatives: Tyrian purple chemistry, physical properties, and their semiconducting characteristics in the solid state [1]. Pitayanatakul et.al. developed 5,5'-dibromoindigo and 5,5'-diphenylindigo which showed excellent ambipolar transistor properties [2]. In another study, they investigated diiodoindigo with the iodine at the 5 position of indigo and this molecule showed excellent

ambipolar transistor properties. They also found that iodine-iodine interaction also affects the ambipolar performance [3]. Klimovich and co-workers synthesized and investigated nine different indigo derivatives for sustainable organic electronics. They solved the degradation problem of Organic Field-Effect Transistors (OFETs) in air, partially by introducing strong electron withdrawing substituents such as two CF<sub>3</sub> groups or four fluorine atoms. They found that, it is necessary to design novel indigoids with further decreased LUMO energy levels down to at least -4.3eV for air stable device operation [4]. Many theoretical researchers have studied the electronic structure and spectroscopic properties of indigo and indigoids. Perpète and Jacquemin performed benchmark calculations for a set of 31 indigoid dyes with 24 functional. They calculated transition energies corresponding to the maximum experimental absorption wavelengths of indigoids at PCM-TD-X/6-311+G(2d,p)//PCM-PBE0/6-311G(d,p) level. They predicted that global hybrids with exact exchange between 20% and 25%, yield the smallest absolute deviation [5]. Amat and co-workers studied the theoretical and experimental investigation on the spectroscopic properties of indigo dye. They evaluated the effects of the intermolecular hydrogen bond in solid state by computing the vibrational spectra of the dimer [6]. Shityakov and co-workers developed a silicon model of indigoid based single electron transistor nanodevices, consisting of indigo and

tyrian purple molecules coupled to gold electrodes by using DFT [7].

Nanostructures as semiconductors are often at the heart of modern optoelectronic devices. Recently, the successful synthesis of single-layer boron (referred to as borophene) opens the era of boron nanostructures. Due to the strong bonding of boron atoms, borophene has high resistance to mechanical impact. One of the unit of borophene sheet ( $B_{36}$ ) consists of 36 boron atoms.  $B_{36}$  is reported as a highly stable cluster with central hexagonal hole in its structure [8,9]. Several adsorption studies of the small gas adsorption of the  $B_{36}$  cluster have been described by theoretical calculation methods [10,11]. Omidvar investigated the sensitivity of the  $B_{36}$  toward two to six hydrogen cyanide (HCN) gas molecule. They found that the  $B_{36}$  is sensitive to the concentrated HCN molecule [10]. Valadbeigi and co-workers studied adsorption of CO,  $N_2$ ,  $H_2O$ ,  $O_2$ ,  $H_2$  and NO molecules on  $B_{36}$  cluster using DFT adopting the B3LYP functional and 6-311+G(d,p) basis set. They found CO,  $O_2$  and NO molecules are adsorbed on the  $B_{36}$  more effectively through formation of chemical bonds. They also indicated that the outer boron atoms of the  $B_{36}$  cluster adsorb the gas molecule better than the inner boron atoms [11]. Kootenaei and co-workers investigated the potential applicability of  $B_{36}$  as electronic sensor for formaldehyde (HCOH) detection by using B97D/6-31G(d) level of theory calculation [12].

Up to the present, no studies have been reported on the adsorption of indigoids on borophene. Borophene and boron clusters are composed of the same elements, and their structural properties are similar to those of graphene and other 2D materials [13]. Based on this similarity, Liu, et al. reported first principles study on the adsorption of gas molecules on borophene [14]. We also assume that borophene may have good adsorption properties for indigoid molecules. The two atoms in the unit cell of borophene have six dispersion branches. The branches of longitudinal acoustic (LA) and Transverse Acoustic (TA) correspond to vibration within the plane, and the other one (ZA) corresponds to out of plane vibration. When compares with graphene, the lifetime of borophene is four orders of magnitude smaller than that dominant ZA modes of graphene. However the lifetimes of LA and TA branches are generally longer than that of ZA, so the LA and TA branches are the main contributors for conductivity of borophene [15]. In this study, we performed first-principles calculations to investigate the adsorption of indigo and indigoid molecules on borophene. The results are expected to provide theoretical support concerning the application of optoelectronic properties in organic semiconducting devices.

### Computational details

We performed all DFT calculations with Gaussian 09 program package [16]. Because of the fact that our indigoid molecules are hypothetical, we used a three steps approach for calculation. In the first step we selected the B3LYP [17] and PBE0 [18] functional and 6-311G(d,p) basis set which are proven for indigoids optimization. TD-DFT calculations [19] were performed with the 6-311+G(2d,p) basis set which uses transition wavelengths for indigoids. The solvation effects

were calculated for chloroform solution Polarizable Continuum Model (PCM) [20] and Conductor-like Polarizable Continuum Model (CPCM) [21]. In the second part, for finding the closest result to the experimental  $I_{\max}$  of indigo in chloroform, B3LYP functional and different basis sets were selected for optimization and TD-DFT calculations. In the third part,  $B_{36}$  borophene and its complexes with indigo and indigoids were carried out using B3LYP functional with a 6-31G(d,p) basis set, a method used earlier for adsorption of molecules on borophene. To check that all structures were in the true local minimum, vibrational frequency analysis was performed with the same level of theory. The adsorption energy is calculated with the following equation:

$$E_{\text{ad}} = E_{\text{indigo}@B_{36}} - E_{\text{indigo}} - E_{B_{36}} \quad (1)$$

where  $E_{\text{indigo}@B_{36}}$  corresponds to the electronic energy of the indigo and indigoids@ $B_{36}$  complex.

Finally TD-DFT calculations for stable structures of indigo and indigoids adsorbed borophene calculated by B3LYP functional and 6-31+(2d,p) basis set.

## Results and discussion

### Absorption spectra of indigo and indigoids

The optimized structures of indigo and indigoids with B3LYP functional and 6-31G(d,p) basis set are shown in Figure 1. To check which functional gives values closer to the experimental absorption spectra of indigo, on the optimized structures in chloroform, the lowest singlet-singlet transitions were computed with B3LYP and PBE0 functional. Table S1 shows the calculated absorption data of indigo with both functional (B3LYP and PBE0) and two different solvation models (PCM and CPCM) in chloroform. The computed transitions were compared with the experimental 285 and 604 nm absorption wavelengths [22]. Both B3LYP and PBE0 functionals gave almost the same values with PCM and CPCM calculations, except from extremely long wavelength. For the 285 nm wavelength, we obtained two closer results, 281, 277 nm and 272, 266 nm from B3LYP and PBE0 functional, respectively. 281 and 272 nm wavelengths have smaller oscillator strength, while 277 and 266 nm wavelengths have stronger oscillator strength. The longest wavelength which originated from the lowest singlet-singlet transition ( $S_0 \rightarrow S_1$ ) was compared with the  $I_{\max}$  at 694 nm of the experimental absorption band. B3LYP showed a deviation of 15 and 10 nm, while PBE0 showed 31 and 27 nm deviation from experimental results with PCM and CPCM solvation models, respectively. Therefore we selected the B3LYP functional for computing the closest result to the experimental  $I_{\max}$  by changing basis set.

Table S2 shows the computed lowest excitations with different basis sets together with the experimental absorption maxima of indigo. The best fit with the experimental data (3nm differences) is found at both B3LYP/6-311+G(2d,p)//B3LYP/6-31G(d,p) and B3LYP/6-311++G(2d,p)//B3LYP/6-31G(d,p) levels in CPCM solvation model. On the other hand, the values from B3LYP/6-31+G(2d,p)//B3LYP/6-31G(d,p) and B3LYP/6-31++G(2d,p)//B3LYP/6-31G(d,p) level showed also closer value

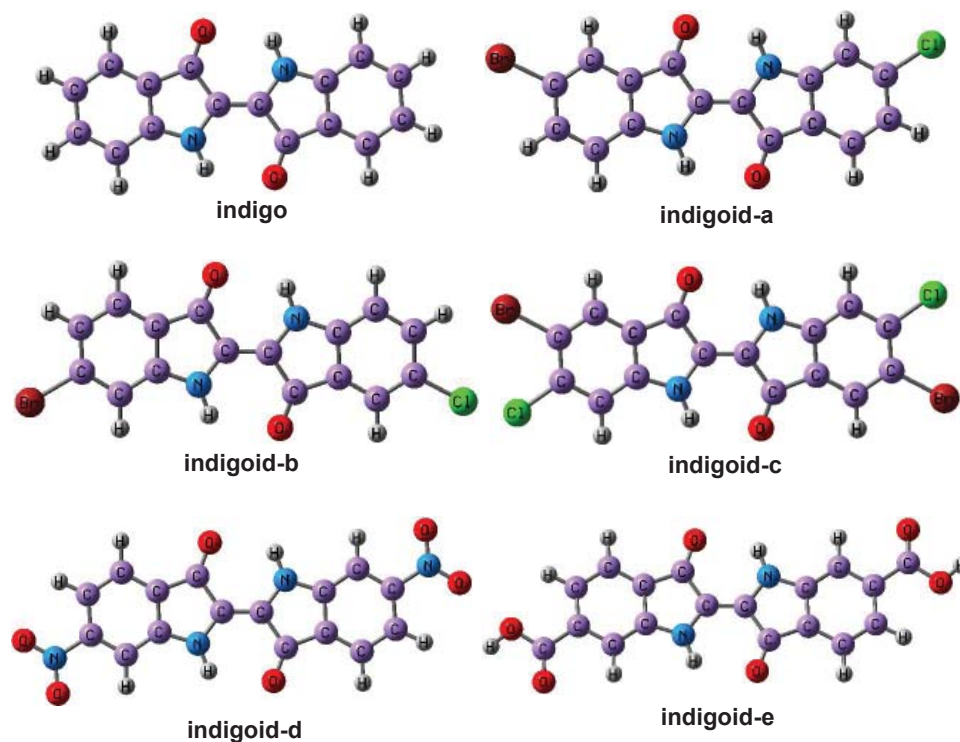


Figure 1: Optimized structures of indigo and indigoids (a,b,c,d,e) at B3LYP/6-31G(d,p) level.

with the experimental ones at 4 nm difference. Due to the large basis set and addition of diffuse functions, there was no influence on the absorption maxima accuracy. Therefore, we selected B3LYP/6-31+G(2d,p)//B3LYP/6-31G(d,p) level of theory for the absorption maxima of our hypothetical indigoid molecules and adsorbed indigo and indigoids on  $B_{36}$ . The selected TD-DFT absorption results of indigo and indigoids with B3LYP functional and 6-31G+(2d,p) basis set are given in Table 1 and spectra are illustrated in Figure 2. Bathochromic shift observed at the  $\lambda_{max}$  of halogen, nitro and carboxylic acid substituted indigoid molecules.

### Adsorption of indigo and indigoids on $B_{36}$

For the adsorption of the indigo and indigoids on  $B_{36}$ , several adsorption states were examined by bonding O atom of indigo and different B atoms of  $B_{36}$  with 1.5Å and 2.0Å bond distances. The indigo was put on  $B_{36}$  surface and edges by lay down or vertical direction. Among all, five stable adsorption states were predicted as shown in Figures 3,4. In the first configuration (indigo@ $B_{36}$ -1), the indigo molecule was put on  $B_{36}$  surface by lay down direction and attached to a boron atom (B6) of the central hexagonal hole. In the second and third configurations (indigo@ $B_{36}$ -2, (indigo@ $B_{36}$ -3), similar to the first configuration, indigo molecule lies on the  $B_{36}$ , but this time the O atom of indigo molecule attached to two different boron atoms (B9 and B31) of the second row of the hexagonal hole. In the fourth configuration (indigo@ $B_{36}$ -4), the indigo molecule attaches from its O atom to the corner B atom (B27) of the edge site of  $B_{36}$  surface. This configuration is the most stable with the adsorption energy of -26.261 kcal/mol (Table 2). The last configuration belongs to the indigo adsorption on the edge site of  $B_{36}$ . In this configuration O atom of the indigo attached to the

Table 1: Selected computed transitions of indigo and indigoids in nm.

Indigo	Indigoid-a	Indigoid-b	Indigoid-c	Indigoid-d	Indigoid-e	Dominant transitions and assignments
				283	274	H→L+4
278	288	287	297	365	304	H-1→L+1
281	289	289	298	424	316	H→L+2
600	605	605	609	683	642	H→L

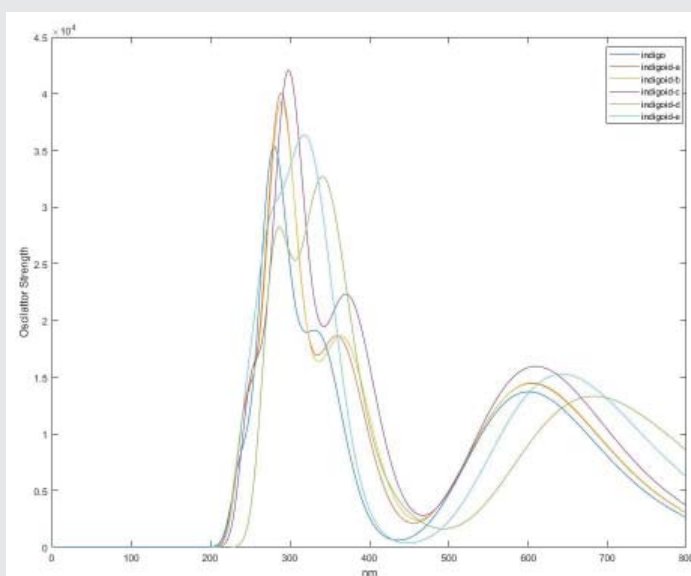


Figure 2: The computed spectra of indigo and indigoids.

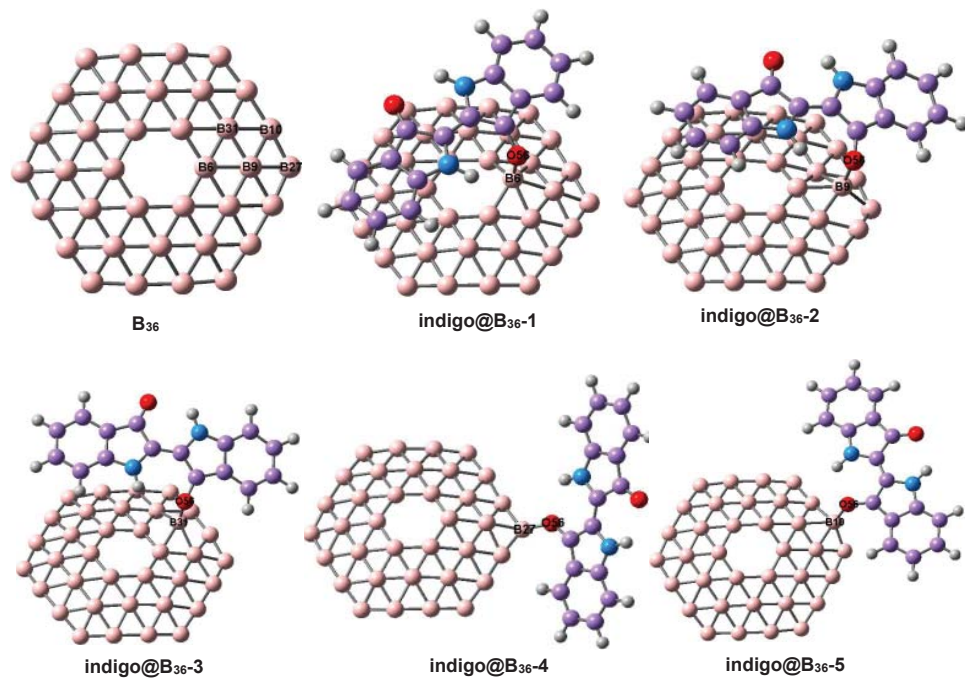


Figure 3: Borophene structure ( $B_{36}$ ) and the stable adsorption states of the  $\text{indigo}@B_{36}$ .

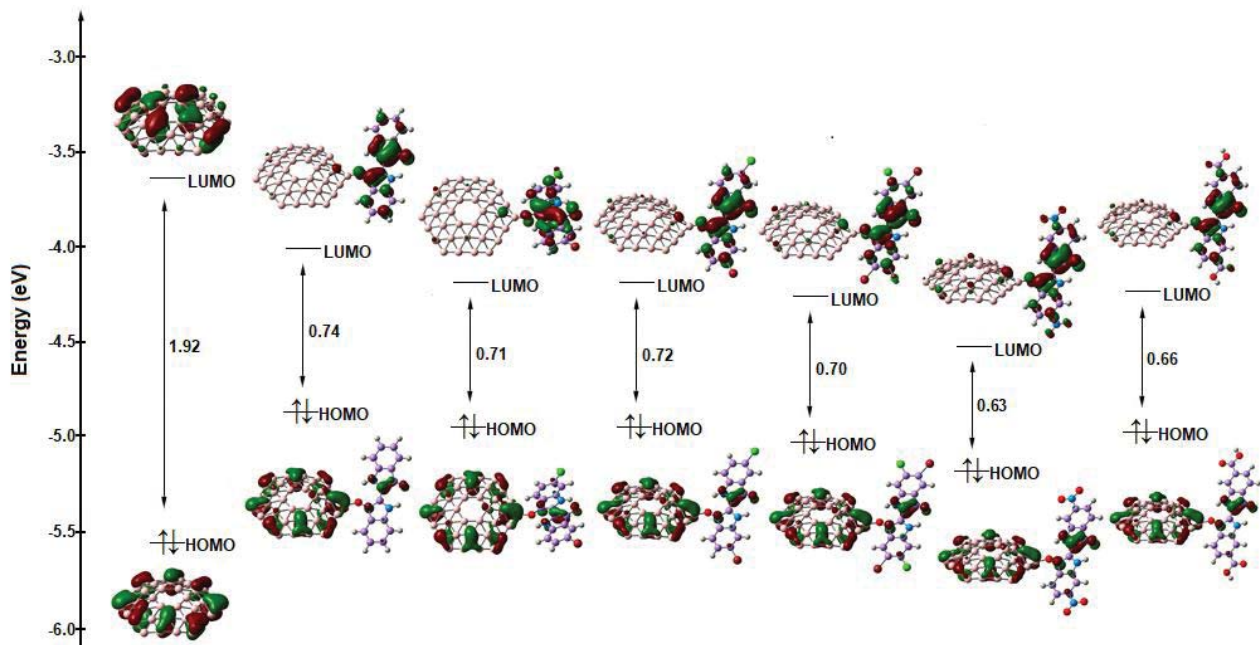


Figure 4: From left to right HOMO and LUMO energies of  $B_{36}$ ,  $\text{indigo}@B_{36}$ ,  $\text{indigoid-a}@B_{36}$ ,  $\text{indigoid-b}@B_{36}$ ,  $\text{indigoid-c}@B_{36}$ ,  $\text{indigoid-d}@B_{36}$ ,  $\text{indigoid-e}@B_{36}$ .

edge site B atom (B18) of  $B_{36}$  surface. Indigoids were also bonded to  $B_{36}$  due to the stable fourth configuration and their energies were calculated. The indigoid-a and indigoid-b were attached to  $B_{36}$  in their two different O sites and then stable structures were selected. Figure 3 depicted HOMO-LUMO gaps and HOMO and LUMO structures of  $B_{36}$  and indigo and indigoids@ $B_{36}$ . As can be seen from the figure, the HOMO-LUMO gap of  $B_{36}$  surface is 1.92 eV. Compared to this, the adsorption process shifts the LUMO level to lower and HOMO level to higher energies with narrowing the HOMO-LUMO gap in all indigo and indigoids@

$B_{36}$  complexes. Because of the fact that the gap of adsorbed indigo and indigoids@ $B_{36}$  structures is in the range of 0.74–0.63 eV, they can be used as narrow energy gap semiconductors [23]. The electrical conductance which is calculated from theoretical computations has been usually simulated by the HOMO-LUMO gap change of semiconductor [24,25]. Based on these studies, the large reduction of HOMO-LUMO gap causes significant increase in the electrical conductance of borophene. As can be seen in Figure 3 the indigoid-d@ $B_{36}$  has the most narrow frontier orbital energy gap and it can be predicted

as a semiconductor with high electrical conductance. In all indigo and indigoids@B<sub>36</sub> structures, while LUMOs are mainly localized on the indigo and indigoids, the HOMOs are localized on the B<sub>36</sub> surface. Because of electron deficiency at this state, the B<sub>36</sub> can be converted to a p-type semiconductor.

### Absorption spectra of indigo and indigoids on B<sub>36</sub>

The impact of indigo and indigoids@B<sub>36</sub> interactions on the adsorbed structures, optical properties are then discussed by TD-DFT. The absorption spectra of indigo and indigoids@B<sub>36</sub> were obtained by using B3LYP/6-31+G(2d,p) level and results are given in Table 3. It can be seen from the **Table S1 and Table S2** indigo and indigoids absorb in the visible region of the spectrum. The absorption spectrum of the B<sub>36</sub> borophene shows a maximum absorption at 452 nm. In comparison between the absorption spectrum of B<sub>36</sub> and its complex with indigo and indigoids, some peaks computed in the visible region and the most intense peak of the complexes found in the near infrared region. In this near infrared absorption region the complexes are suitable as heat adsorber [26]. The absorption wavelengths and dominant electronic transitions with their assignments are also listed in Table 3. It can be seen from the table that the maximum absorptions for the complexes occurs in the range 1640 to 1683 nm with HOMO→LUMO transition. It is shown that this HOMO→LUMO transition is directly due to photoinduced

**Table 2:** The stable energies and adsorption energies of the indigo@B<sub>36</sub>

	Energies (hartree)	E <sub>ads</sub> (kcal/mol)
B <sub>36</sub>	-894.3375536	
indigo	-875.716107	
indigo@B <sub>36</sub> -1	-1770.058468	-3.017
indigo@B <sub>36</sub> -2	-1770.065745	-7.583
indigo@B <sub>36</sub> -3	-1770.066050	-7.774
indigo@B <sub>36</sub> -4	-1770.095511	-26.261
indigo@B <sub>36</sub> -5	-1770.059402	-3.603

**Table 3:** Selected computed transitions wavelengths of indigo@B<sub>36</sub> and indigoids@B<sub>36</sub> in nm.

B <sub>36</sub>	indigo@B <sub>36</sub>	Indigoid-a@B <sub>36</sub>	Indigoid-b@B <sub>36</sub>	Indigoid-c@B <sub>36</sub>	Indigoid-d@B <sub>36</sub>	Indigoid-e@B <sub>36</sub>	Dominant transitions and assignments
449 <sup>a</sup>	634	651	647	663	657	680	H-5→L (° H-4→L)
	767	775	774	791	826	808	H-3→L
	889	900	897	910	935	928	H-2→L
	1660	1650	1645	1640	1659	1683	H→L

### References

- Głowacki ED, Voss G, Leonat L, Irimia-Vladu M, Bauer S, et al. (2012) Indigo and Tyrian Purple – From Ancient Natural Dyes to Modern Organic Semiconductors. *Isr J Chem* 52: 540-551. [Link: https://bit.ly/3u4cOrG](https://bit.ly/3u4cOrG)
- Pitayatanakul O, Higashino T, Kadoya T, Tanaka M, Kojima H, et al. (2014) High performance ambipolar organic field-effect transistors based on indigo derivatives. *J Mater Chem C* 2: 9311-9317. [Link: https://rsc.li/3dclLXX](https://rsc.li/3dclLXX)
- Pitayatanakul O, Iijima K, Ashizawa M, Kawamoto T, Matsumoto H, et al. (2015) An Iodine Effect in Ambipolar Organic Field-effect Transistors Based on Indigo Derivatives. *J Mater Chem C* 3: 8612–8617. [Link: https://rsc.li/3swZ5cv](https://rsc.li/3swZ5cv)

charge transfer phenomena as the electron density of the HOMO is located on the B<sub>36</sub> and that of the LUMO is located on the indigo and indigoid molecules. The absorptions in the visible region (from 630 to 680 nm) associated with the H-5→L transitions emphasize the importance of these complexes in solar cell devices [27].

### Conclusion

Borophene brings a new member to the magnificent 2D materials family and opens the way to exploring the boron-based microelectronic devices. However, the research of borophene is just in its beginning, and a lot of properties remain to be explored before borophene can be established as a valuable alternative for the next generation of electronic applications. To improve the performance of semiconductor behavior of borophene, we conducted the first principle study of the adsorption of indigo and indigoids on a B<sub>36</sub> borophene surface. After the adsorption of indigo molecule on the B<sub>36</sub>, considering six different configurations, the strongest adsorption configuration of indigo was found on the edge of B<sub>36</sub>. Five different indigoids molecule conducted this edge adsorption configuration of B<sub>36</sub>. Due to indigo and indigoids@B<sub>36</sub> adsorption process, we found that the HOMO-LUMO gap of B<sub>36</sub> is considerably decreased. Using TD-DFT method the absorption spectra of indigo and indigoids@B<sub>36</sub> were obtained from visible to near infrared region. From the absorption wavelengths of the indigo and indigoids@B<sub>36</sub> complexes, the charge transfer transitions were observed in the near infrared and visible regions. The findings of this study suggests that the B<sub>36</sub> borophene structures can be used as organic semiconducting devices whose electronic conduction vary because of the interaction of indigo and indigoid molecules.

### Acknowledgment

The presented numerical results were obtained at TUBITAK ULAKBIM, High Performance and Grid Computing Center (TRUBA Resources).

- Klimovich IV, Leshanskaya LI, Troyanov SI, Anokhin DV, Novikov DV, et al. (2014) Design of indigo derivatives as environment-friendly organic semiconductors for sustainable organic electronics. *J Mater Chem C* 2: 7621–7631. [Link: https://rsc.li/2P8sgEs](https://rsc.li/2P8sgEs)
- Perpète EA, Jacquemin D (2009) TD-DFT benchmark for indigoid dyes. *Journal of Molecular Structure: THEOCHEM* 914: 100-105. [Link: https://bit.ly/2PEEgNO](https://bit.ly/2PEEgNO)
- Amat A, Rosi F, Miliani C, Sgamellotti A, Fantacci S (2011) Theoretical and experimental investigation on the spectroscopic properties of indigo dye. *Journal of Molecular Structure* 993: 43-51. [Link: https://bit.ly/2P8spru](https://bit.ly/2P8spru)
- Shityakov S, Roewer N, Förster C, Broscheit JA (2017) In Silico Modeling of

- Indigo and Tyrian Purple Single-Electron Nano-Transistors Using Density Functional Theory Approach. *Nanoscale Research Letters* 12: 439-446. [Link: https://bit.ly/31pA86W](https://bit.ly/31pA86W)
8. Piazza ZA, Hu HS, Li WL, Li YF, Zhao J, et al. (2014) Planar hexagonal B36 as a potential basis for extended single-atom layer boron sheets. *Nat Commun* 5: 3113-3122. [Link: https://go.nature.com/3wh457x](https://go.nature.com/3wh457x)
9. Chen Q, Wei GF, Tian WJ, Bai H, Liu ZP, et al. (2014) Quasi-planar aromatic B36 and B36- clusters: all-boron analogues of coronene. *Phys Chem Chem Phys* 16: 18282-1887. [Link: https://rsc.li/3djlPGI](https://rsc.li/3djlPGI)
10. Omidvar A (2017) Borophene: A novel boron sheet with a hexagonal vacancy offering high sensitivity for hydrogen cyanide detection. *Computational and Theoretical Chemistry* 1115: 179-184. [Link: https://bit.ly/3swQMNH](https://bit.ly/3swQMNH)
11. Valadbeigi Y, Farrokhpour H, Tabrizchi M (2015) Adsorption of small gas molecules on B36 nanocluster. *J Chem Sci* 127: 2029-2038. [Link: https://bit.ly/3cxrOzi](https://bit.ly/3cxrOzi)
12. Kootenaei AS, Ansari G (2016) B36 borophene as an electronic sensor for formaldehyde: Quantum chemical analysis. *Physics Letters A* 380: 2664-2668. [Link: https://bit.ly/3u2Ybol](https://bit.ly/3u2Ybol)
13. a) Lherbier A, Botello-Méndez AR, Charlier JC (2016) Electronic and optical properties of pristine and oxidized borophene. *2D Mater* 3: 045006. [Link: https://bit.ly/3rxAMtN](https://bit.ly/3rxAMtN)
- b) Padilha JE, Miwa RH, Fazzio A (2016) Directional dependence of the electronic and transport properties of 2D borophene and borophane. *Phys Chem Chem Phys* 18: 25491-25496. [Link: https://rsc.li/3cupmm0](https://rsc.li/3cupmm0)
- c) Mortazavi B, Rahaman O, Dianat A, Rabczuk T (2016) Mechanical responses of borophene sheets: a first-principles study. *Phys Chem Chem Phys* 18: 27405-27413. [Link: https://rsc.li/3cxCMOh](https://rsc.li/3cxCMOh)
- d) Wang H, Li Q, Gao Y, Miao F, Zhou XF, et al. (2016) Strain effects on borophene: ideal strength, negative Poisson's ratio and phonon instability. *New J Phys* 18: 073016. [Link: https://bit.ly/2QF4fVG](https://bit.ly/2QF4fVG)
- e) Liu Y, Dong YJ, Tang Z, Wang XF, Wang L, et al. (2016) Stable and metallic borophene nanoribbons from first-principles calculations. *J Mater Chem C* 4: 6380-6385. [Link: https://rsc.li/3syIG7s](https://rsc.li/3syIG7s)
14. Liu T, Chen Y, Zhang M, Yuan L, Zhang C, et al. (2017) A first-principles study of gas molecule adsorption on borophene. *AIP Advances* 7: 125007-1-125007-9. [Link: https://bit.ly/3lYoAkY](https://bit.ly/3lYoAkY)
15. Yang Z, Yuan K, Menga J, Hu M (2020) Electric field tuned anisotropic to isotropic thermal transport transition in monolayer borophene without altering its atomic structure. *Nanoscale* 12: 19178-19190. [Link: https://rsc.li/3w3QINJ](https://rsc.li/3w3QINJ)
16. Frisch MJ, Trucks GW, Schlegel HB, Scuseria GE, Robb MA, et al. (2009) Gaussian 09, Revision C.1, Gaussian, Inc., Wallingford CT.
17. a) Becke AD (1993) Density-functional thermochemistry. III. The role of exact exchange. *J Chem Phys* 98: 5648-5652. [Link: https://bit.ly/3w8rbqj](https://bit.ly/3w8rbqj)
- b) Lee C, Yang W, Parr RG (1988) Development of the Colle-Salvetti correlation-energy formula into a functional of the electron density. *Phys Rev B* 37: 785-789. [Link: https://bit.ly/3w60YyZ](https://bit.ly/3w60YyZ)
18. Adamo C, Barone V (1999) Toward reliable density functional methods without adjustable parameters: The PBE0 model. *J Chem Phys* 110: 6158-6169. [Link: https://bit.ly/3lYpgX8](https://bit.ly/3lYpgX8)
19. a) Cossi M, Scalmani G, Rega N, Barone V (2002) New developments in the polarizable continuum model for quantum mechanical and classical calculations on molecules in solution. *J Chem Phys* 117: 43-54. [Link: https://bit.ly/3mCuQW5](https://bit.ly/3mCuQW5)
- b) Tomasi J, Mennucci B, Cammi R (2005) Quantum Mechanical Continuum Solvation Models. *Chem Rev* 105: 2999-3093. [Link: https://bit.ly/3tWXuNk](https://bit.ly/3tWXuNk)
20. a) Stratmann RE, Scuseria GE, Frisch MJ (1998) An efficient implementation of time-dependent density-functional theory for the calculation of excitation energies of large molecules. *J Chem Phys* 109: 8218-8224. [Link: https://bit.ly/3fk850R](https://bit.ly/3fk850R)
- b) Matsuzawa NN, Ishitani A, Dixon DA, Uda T (2001) Time-Dependent Density Functional Theory Calculations of Photoabsorption Spectra in the Vacuum Ultraviolet Region. *J Phys Chem A* 105: 4953-4962. [Link: https://bit.ly/3cyCabj](https://bit.ly/3cyCabj)
- c) Casida ME, Jamorski C, Casida KC, Salahub DR (1998) Molecular excitation energies to high-lying bound states from time-dependent density-functional response theory: Characterization and correction of the time dependent local density approximation ionization threshold. *J Chem Phys* 108: 4439-4449. [Link: https://bit.ly/39mfjxm](https://bit.ly/39mfjxm)
21. a) Barone V, Cossi M (1998) Quantum calculation of molecular energies and energy gradients in solution by a conductor solvent model. *J Phys Chem A* 102: 1995-2001. [Link: https://bit.ly/2PeQRr3](https://bit.ly/2PeQRr3)
- b) Cossi M, Rega N, Scalmani G, Barone V (2003) Energies, structures, and electronic properties of molecules in solution with the C-PCM solvation model. *J Comp Chem* 24: 669-681. [Link: https://bit.ly/3rwH500](https://bit.ly/3rwH500)
22. Brode WR, Pearson EG, Wyman GM (1954) The Relation between the Absorption Spectra and the Chemical Constitution of Dyes. XXVII. cis-trans Isomerism and Hydrogen Bonding in Indigo Dyes. *J Am Chem Soc* 76: 1034-1036. [Link: https://bit.ly/3dg5a6H](https://bit.ly/3dg5a6H)
23. Joshi A, Ramachandran CN (2018) Structural, optoelectronic and charge transport properties of the complexes of indigo encapsulated in carbon nanotubes. *Phys Chem Chem Phys* 20: 15158-15167. [Link: https://rsc.li/31wMkCE](https://rsc.li/31wMkCE)
24. Hadipour NL, Peyghan AA, Soleymanabadi H (2015) Theoretical Study on the Al-Doped ZnO Nanoclusters for CO Chemical Sensors. *J Phys Chem C* 119: 6398-6404. [Link: https://bit.ly/3flRSbx](https://bit.ly/3flRSbx)
25. Kootenaei AS, Ansari G (2016) B36 borophene as an electronic sensor for formaldehyde: Quantum chemical analysis. *Physics Letters A* 380: 2664-2668. [Link: https://bit.ly/3deMNYT](https://bit.ly/3deMNYT)
26. Qian G, Wang ZY (2010) Near-Infrared Organic Compounds and Emerging Applications. *Chem Asian J* 5: 1006-1029. [Link: https://bit.ly/3lZaXsd](https://bit.ly/3lZaXsd)
27. Ghann W, Kang H, Sheikh T, Yadav S, Chavez-Gil T, et al. (2017) Fabrication, Optimization and Characterization of Natural Dye Sensitized Solar Cell. *Sci Rep* 7: 41470-41481. [Link: https://go.nature.com/3fnaxDV](https://go.nature.com/3fnaxDV)